ELectronics EXpress

IEICE Electronics Express, Vol.17, No.7, 1–4

LETTER

Multiple-model hybrid particle/FIR filter for indoor localization using wireless sensor networks

Jung Min Pak[1a)]

Abstract This letter proposes a new state estimator called the multiple-model hybrid particle/finite-impulse-response (FIR) filter (MMHPFF) for indoor localization using wireless sensor networks. In the proposed hybrid filtering algorithm, the multiple-model particle filter has the role of the main filter, and it overcomes uncertain process noise problems arising from the use of the constant velocity (CV) motion model in indoor localization. In addition, the multiple-model FIR filter is used as an assisting filter to overcome particle filter failures owing to the sample impoverishment phenomenon. Indoor localization simulations demonstrated that the proposed MMHPFF is more accurate and reliable than conventional algorithms.

Keywords: finite-impulse-response (FIR) filter, indoor localization, multiple-model filtering, particle filter, wireless sensor network

Classification: Microwave and millimeter-wave devices, circuits, and modules

1. Introduction

Indoor localization systems based on wireless sensor networks (WSNs) have been used widely for real-time position monitoring of humans, robots, and equipment in various facilities [1, 2, 3, 4, 5, 6, 7, 8, 9, 10, 11, 12, 13, 14, 15]. A WSN for indoor localization is composed of several fixed and mobile nodes. Fixed nodes are installed at fixed positions in an indoor space, and mobile nodes are attached to tracked target objects. Wireless communication technologies for WSN include radio-frequency identification (RFID) [5, 6], ultra-wide band (UWB) [7, 8, 9, 10], and chirp spread spectrum (CSS) [11]. Localization systems can exploit various wireless measurements including the time of arrival (TOA) [12], the time difference of arrival (TDOA) [13], and the angle of arrival (AOA) [10]. To obtain target positions from noisy measurements, state estimators (also called stochastic filters) are typically used [3, 5, 6, 9, 11, 13]. State estimators estimate state variables (e.g., positions and velocities) using system state-space models and noisy measurements [16].

The particle filter (PF) is one of the most widely used state estimators and has advantages in nonlinear state estimation problems including indoor localization using WSNs. However, the PF has the disadvantage in that the PF algorithm fails if the sample impoverish phenomenon occurs under the harsh conditions of a small number of particles or low measurement noise [17]. To overcome this problem, the hybrid particle/finite-impulse-response (FIR) filters (HPFFs) [14, 15] were proposed. In the HPFF algorithm, the PF has a role of the main filter. When PF algorithm fails under the harsh conditions mentioned above, the assisting FIR filter operates to recover the main filter from failures. The FIR filter [18, 19, 20, 21, 22, 23, 24, 25, 26, 27] is generally less accurate than the PF in nonlinear state estimation problems; however, it has intrinsic robustness against model uncertainty and bounded-input bounded-output (BIBO) stability. Thus, the FIR filter is appropriate for the role of the assisting filter that operates under harsh conditions.

In the state estimation for indoor localization, the constant velocity (CV) motion model is typically used to represent the motion of target objects. In the CV model, the process noise covariance **Q** plays a critical role; however, it is a very uncertain design parameter [28]. Thus, inappropriately selected **Q** values may worsen localization accuracy [20, 26, 27]. In cases where state-space models have uncertainties, multiple-model approaches have been commonly used [16, 17, 28]. Therefore, this letter proposes a new state estimator that exploits the multiple-model approach to overcome the uncertain process noise problem in the use CV motion model for indoor localization. The proposed estimator is called the multiple-model hybrid particle/finite-impulse-response (FIR) filter (MMHPFF), which is obtained by extending the HPFF to the multiple-model filtering. In the MMHPFF algorithm, the multiple-model PF (MMPF) [29, 30, 31] is used as a main filter and it can overcome the problem of the uncertain process noise model. When MMPF failures occur, the assisting MMFF operates to recover the main filter from failures. The recovery process is performed by resetting and rebooting the MMPF using the output of the MMFF. Indoor localization simulations demonstrate that the MMHPFF provides more accurate and reliable localization than the single-model PF and the MMPF.

2. Multiple-model hybrid particle/FIR filter for indoor localization

We consider two-dimensional (2D) indoor floor space to simplify the problem. Four receivers (fixed nodes) are installed at the corners of a rectangular-shaped space, and a transmitter (mobile node) is attached to a human moving

[1]Department of Electrical Engineering, Wonkwang University, 460 Iksandae-ro, Iksan, Jeonbuk, 54538, Republic of Korea
a) destin11@wku.ac.kr

DOI: 10.1587/elex.17.20200020
Received January 15, 2020
Accepted March 9, 2020
Publicized March 24, 2020
Copyedited April 10, 2020

in the space. The TOAs measured at a discrete time step k are represented as follows:

$$z_{i,k} = \frac{1}{c}\sqrt{(x_k - x_i)^2 + (y_k - y_i)^2} + v_k, \tag{1}$$

where $z_{i,k}$ is the TOA obtained from the i-th receiver, c is the speed of light, (x_k, y_k) and (x_i, y_i) are 2D coordinates of the human (transmitter) and the i-th receiver, respectively, and v_k is the zero-mean white Gaussian measurement noise with variance $\mathbf{r}$.

State estimators estimate the human position using the noisy TOA measurements and the state-space models. We use the CV motion model, where the state vector consists of 2D coordinates and velocities as $\mathbf{x}_k = [x_k\ y_k\ \dot{x}_k\ \dot{y}_k]^T$. The CV motion model describes the state transition as follows:

$$\mathbf{x}_k = \mathbf{A}\mathbf{x}_{k-1} + \mathbf{G}\mathbf{w}_{k-1}, \tag{2}$$

$$\mathbf{A} = \begin{bmatrix} 1 & 0 & T & 0 \\ 0 & 1 & 0 & T \\ 0 & 0 & 1 & 0 \\ 0 & 0 & 0 & 1 \end{bmatrix}, \quad \mathbf{G} = \begin{bmatrix} \frac{T^2}{2} & 0 \\ 0 & \frac{T^2}{2} \\ T & 0 \\ 0 & T \end{bmatrix}, \tag{3}$$

where $\mathbf{w}_{k-1} \in \Re^2$ is the zero-mean white Gaussian process noise vector with the covariance $\mathbf{Q}_{k-1}$, and T is the sampling interval. $\mathbf{Q}$ is a key parameter reflecting target motion (course and speed); however, motion of a human is unpredictable and $\mathbf{Q}$ is a highly uncertain parameter. Therefore, the MMHPFF is proposed to overcome the model uncertainty. The TOA measurement model is represented as

$$\mathbf{z}_k = \mathbf{h}_k(\mathbf{x}_k) + \mathbf{v}_k, \tag{4}$$

where $\mathbf{z}_k = [z_{1,k}\ z_{2,k}\ z_{3,k}\ z_{4,k}]^T$ and $\mathbf{h}_k(\cdot)$ is the vector representation of the nonlinear function in (1). The measurement noise covariance matrix is $\mathbf{R} = \mathbf{r}\mathbf{I}_4$, where $\mathbf{I}_4$ indicates the 4×4 identity matrix.

The MMHPFF uses the MMPF as a main filter. The MMPF adopts the regime (model) variable r_k as a new state variable, and r_k is in effect during the time interval $(t_{k-1}, t_k]$. Thus, the augmented state vector is defined as $\mathbf{y}_k = [\mathbf{x}_k^T\ r_k]^T$, where $r_k \in S = \{1, 2, \cdots, s\}$ and s indicates the number of models. The multiple CV motion models are constructed by selecting several $\mathbf{Q}$ values, and $\mathbf{Q}_k$ at time k becomes a function of r_k as $\mathbf{Q}_k^{(r_k)}$.

The first step of the MMPF algorithm is to generate the random set $\{r_k^p\}_{p=1}^N$, where N is the number of particles (samples), based on $\{r_{k-1}^p\}_{p=1}^N$ and the transition probability matrix (TPM) denoted by Π [17]. The next step is the regime conditioned sampling process, where the state transition is performed using the multiple CV motion models determined by the regime variable as

$$\mathbf{x}_k^p = \mathbf{A}\mathbf{x}_{k-1}^p + \mathbf{G}\mathbf{w}_{k-1}^p, \tag{5}$$

$$\mathbf{w}_{k-1}^p \sim \mathcal{N}(0, \mathbf{Q}_{k-1}^{(r_k^p)}), \tag{6}$$

where $\mathcal{N}(0, \mathbf{Q}_{k-1}^{(r_k^p)})$ indicates the Gaussian density with the mean 0 and the covariance $\mathbf{Q}_{k-1}^{(r_k^p)}$). The last step is the resampling process, which is almost the same as that of the generic (single model) PF. The only difference is to find a dominant regime at each time step. r_k with the greatest portion is selected as the dominant regime r_k^*. The MMPF produces the output, $\hat{\mathbf{y}}_k = [\hat{\mathbf{x}}_k^T\ r_k^*]^T$, where $\hat{\mathbf{x}}_k$ is obtained by computing sample mean of the particles.

The MMHPFF uses the MMFF as an assisting filter that operates only when a MMPF failure is detected. The MMFF uses only recent finite measurements on the time interval $[m, n]$, where m and n are defined as $m = k - M + 1$ and $n = k - 1$, respectively, and M is the memory size. The MMFF produces the estimated state $\hat{\mathbf{x}}_k^*$ and the estimation error covariance $\mathbf{P}_k^*$, which are computed as follows:

$$\hat{\mathbf{x}}_k^* = \mathbf{L}\mathbf{Z}_M, \tag{7}$$

$$\mathbf{P}_k^* = \mathbf{K}_M\mathbf{Q}_M\mathbf{K}_M^T + \mathbf{L}\mathbf{R}_M\mathbf{L}^T, \tag{8}$$

$$\mathbf{L} = \mathbf{J}_M \begin{bmatrix} \mathbf{W}_{1,1} & \mathbf{W}_{1,2} \\ \mathbf{W}_{1,2}^T & \mathbf{W}_{2,2} \end{bmatrix}^{-1} \begin{bmatrix} \bar{\mathbf{H}}_N^T \\ \bar{\mathbf{G}}_N^T \end{bmatrix} \mathbf{R}_M^{-1}, \tag{9}$$

$$\mathbf{J}_M = [\mathbf{A}^M\ \mathbf{A}^{M-1}\ \mathbf{A}^{M-2}\ \cdots\ \mathbf{A}\ \mathbf{I}], \tag{10}$$

$$\mathbf{W}_{1,1} = \bar{\mathbf{H}}_M^T\mathbf{R}_M^{-1}\bar{\mathbf{H}}_M, \tag{11}$$

$$\mathbf{W}_{1,2} = \bar{\mathbf{H}}_M^T\mathbf{R}_M^{-1}\bar{\mathbf{G}}_M, \tag{12}$$

$$\mathbf{W}_{2,2} = \bar{\mathbf{G}}_M^T\mathbf{R}_M^{-1}\bar{\mathbf{G}}_M + \mathbf{Q}_M^{-1}, \tag{13}$$

$$\bar{\mathbf{H}}_M = \begin{bmatrix} \mathbf{H}_m \\ \mathbf{H}_{m+1}\mathbf{A} \\ \mathbf{H}_{m+2}\mathbf{A}^2 \\ \vdots \\ \mathbf{H}_n\mathbf{A}^{M-1} \end{bmatrix}, \quad \mathbf{H}_m = \left.\frac{\partial \mathbf{h}_m}{\partial \mathbf{x}_m}\right|_{\hat{\mathbf{x}}_m}, \tag{14}$$

$$\bar{\mathbf{G}}_M = \begin{bmatrix} \mathbf{0} & \mathbf{0} & \dots & \mathbf{0} & \mathbf{0} \\ \mathbf{H}_{m+1} & \mathbf{0} & \dots & \mathbf{0} & \mathbf{0} \\ \mathcal{H}_{m+2,m+1} & \mathbf{H}_{m+2} & \dots & \mathbf{0} & \mathbf{0} \\ \vdots & \vdots & \vdots & \vdots & \vdots \\ \mathcal{H}_{n,m+1} & \mathcal{H}_{n,m+2} & \dots & \mathbf{H}_n & \mathbf{0} \end{bmatrix}, \tag{15}$$

$$\mathcal{H}_{g,h} = \mathbf{H}_g\mathbf{A}^{h-g-2} \quad (g > h), \tag{16}$$

$$\mathbf{R}_M = [\mathrm{diag}(\overbrace{\mathbf{R}\ \mathbf{R}\ \cdots\ \mathbf{R}}^{M})], \tag{17}$$

$$\mathbf{Q}_M = [\mathrm{diag}(\overbrace{\mathbf{Q}_m^{(r_m^*)}\ \mathbf{Q}_{m+1}^{(r_{m+1}^*)}\ \cdots\ \mathbf{Q}_n^{(r_n^*)}}^{M})], \tag{18}$$

$$\mathbf{Z}_M = [\mathbf{z}_m^T\ \mathbf{z}_{m+1}^T\ \cdots\ \mathbf{z}_n^T]^T, \tag{19}$$

$$\mathbf{K}_M = [\mathbf{A}^{M-1}\mathbf{G}\ \mathbf{A}^{M-2}\mathbf{G}\ \cdots\ \mathbf{A}\mathbf{G}\ \mathbf{G}]. \tag{20}$$

Note that the outputs of the MMPF were used for MMFF in (14) and (18).

The key idea of the hybrid particle/FIR filtering is to detect PF failures and to reset the PF using the output of the FIR filter. Failure detection is performed based on the Mahalanobis distance [32] between the predicted measurement $\hat{\mathbf{z}}_k$ and the actual measurement $\mathbf{z}_k$, which is computed as

$$\mathcal{D}_k = (\mathbf{z}_k - \hat{\mathbf{z}}_k)\mathbf{R}^{-1}(\mathbf{z}_k - \hat{\mathbf{z}}_k), \quad \hat{\mathbf{z}}_k = \mathbf{h}_k(\hat{\mathbf{x}}_k). \tag{21}$$

If $\mathcal{D}_k$ is greater than a predetermined threshold χ^2, we judge that main filter failure occurs. The threshold χ^2 is taken from the chi-square table [33]. For example, the 4th degree system having four measurements requires $\chi^2 = 13.28$ for the confidence level of 99%. When the MMPF failure is detected, the assisting MMFF operates and produces $\hat{\mathbf{x}}_k^*$ and $\mathbf{P}_k^*$. Next, the random samples are generated as $\hat{\mathbf{x}}_{k,p} \sim \mathcal{N}(\hat{\mathbf{x}}_k^*, \mathbf{P}_k^*)$, $(p = 1, 2, \cdots, N)$. Additionally, a random set of regime values $\{r_k^p\}_{p=1}^N$ is generated following the discrete uniform distribution. Lastly, the main MMPF is reset using the new sample set $\{\hat{\mathbf{x}}_{k,p}^T \; r_k^p\}_{p=1}^N$.

3. Simulation

We demonstrated the proposed MMHPFF using indoor localization simulations. Four receivers were installed at the corners and a human with a transmitter traveled along a square-shaped trajectory as shown in Fig. 1. At each time step k, 2D positions of the human were estimated using the state estimators, such as the MMHPFF, MMPF, and PF. For the multiple CV motion models, we choose three $\mathbf{Q}$ values as $\mathbf{Q}^{(1)} = 0.1^2\mathbf{I}_2$, $\mathbf{Q}^{(2)} = \mathbf{I}_2$, and $\mathbf{Q}^{(3)} = 10^2\mathbf{I}_2$. The MMHPFF and the MMPF used the multiple CV motion models, where the TPM was set as

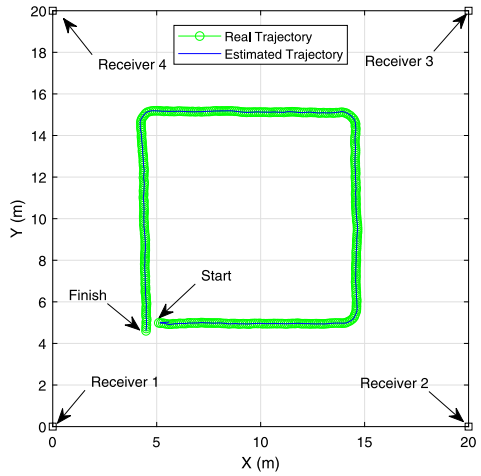

Fig. 1. Schematic of indoor localization simulation.

$$\Pi = \begin{bmatrix} 0.9 & 0.09 & 0.01 \\ 0.1 & 0.8 & 0.1 \\ 0.01 & 0.09 & 0.9 \end{bmatrix}. \tag{22}$$

The PF used three (single) CV models and each of them matched to the three $\mathbf{Q}$ values mentioned above. The memory size of the assisting MMFF in the MMHPFF was set as $M = 4$. The simulation time was $40s$ and the sampling interval was set as $T = 0.1s$. Thus, a simulation performed during $1 \le k \le 400$. The localization performance was evaluated using the total localization error (TLE) computed as

$$\mathbf{TLE} = \frac{1}{400}\sum_{k=1}^{400}\sqrt{(x_k - \hat{x}_k)^2 + (y_k - \hat{y}_k)^2}, \tag{23}$$

where (x_k, y_k) and $(\hat{x}_k, \hat{y}_k)$ are the true and estimated 2D coordinates (unit: meter) of the human. We ran 100 MC simulations and computed the averaged TLE (ATLE) for the effective MC simulations. We judged that an MC simulation that TLE exceeds $5m$ is a localization failure and discarded it when computing the ATLE.

Simulations were performed under three different conditions. The first simulation was performed under normal conditions, where we set the measurement noise covariance and the number of particles as $\mathbf{R} = 0.5^2\mathbf{I}_4$ and $N = 100$, respectively. The second and the third simulations were performed under harsh conditions, such as small number of particles ($N = 20$ and $\mathbf{R} = 0.5^2\mathbf{I}_4$) and low measurement noise ($N = 100$ and $\mathbf{R} = 0.1^2\mathbf{I}_4$). Accuracy and reliability of the algorithms were evaluated using ATLE and the number of localization failures N_F, respectively. Simulation results are shown in Table I, where "-" indicates that ATLE cannot be computed because $N_{\text{fail}} = 100$. In Table I, the MMHPFF shows a lower ATLE and N_{fail} than the other algorithms. In the simulation, $\mathbf{Q}^{(3)}$ was the best choice for the single-model PF; however, the choice is difficult. Note that the MMHPFF provides better performance that single-model PFs without choice of $\mathbf{Q}$.

Table I. Simulation results.

Algorithms	Normal		Small N		Low $\mathbf{R}$	
	ATLE	N_F	ATLE	N_F	ATLE	N_F
MMHPFF	0.026	0	0.050	0	0.116	0
MMPF	0.027	0	0.062	0	1.173	99
PF with $\mathbf{Q}^{(1)}$	1.015	19	2.683	96	-	100
PF with $\mathbf{Q}^{(2)}$	0.039	0	0.072	0	1.083	96
PF with $\mathbf{Q}^{(3)}$	0.027	0	0.062	0	-	100

4. Conclusion

This letter proposed a new state estimator called the MMHPFF for indoor localization using WSNs. The MMHPFF overcomes uncertainty of the process noise covariance of the CV motion model. In addition, the MMHPFF is robust against PF failures owing to the recovery process using the assisting MMFF. Simulation results demonstrated that the MMHPFF is more accurate and reliable than both the PF and MMPF. Therefore the MMHPFF is suitable for indoor localization in various industrial applications.

Acknowledgments

This paper was supported by Wonkwang University in 2018.

References

[1] H. Liu, *et al.*: "Survey of wireless indoor positioning technique and systems," IEEE Trans. Syst., Man, Cybern. C **37** (2007) 1067 (DOI: 10.1109/TSMCC.2007.905750).
[2] M. S. Karoui, *et al.*: "A compact UWB elliptic antenna for indoor localization system," IEICE Electron. Express **16** (2019) 20190425 (DOI: 10.1587/elex.16.20190425).
[3] L. Cheng, *et al.*: "Mobile location estimation scheme in NLOS environment," IEICE Electron. Express **8** (2011) 1829 (DOI: 10.1587/elex.8.1829).

[4] Q. Shi, *et al.*: "A 3D node localization scheme for wireless sensor networks," IEICE Electron. Express **6** (2009) 167 (DOI: 10.1587/elex.6.167).
[5] E. DiGiampaolo and F. Martinelli: "Mobile robot localization using the phase of passive UHF-RFID signals," IEEE Trans. Ind. Electron. **61** (2014) 365 (DOI: 10.1109/TIE.2013.2248333).
[6] P. Yang and W. Wu: "Efficient particle filter localization algorithm in dense passive RFID tag environment," IEEE Trans. Ind. Electron. **61** (2014) 5641 (DOI: 10.1109/TIE.2014.2301737).
[7] D. B. Jourdan, *et al.*: "Position error bound for UWB localization in dense cluttered environments," IEEE Trans. Aerosp. Electron. Syst. **44** (2008) 613 (DOI: 10.1109/TAES.2008.4560210).
[8] Z. Li, *et al.*: "A 3-tier UWB-based indoor localization systems for ultra-low-power sensor network," IEEE Trans. Wireless Commun. **8** (2009) 2813 (DOI: 10.1109/TWC.2009.080602).
[9] J. González, *et al.*: "Mobile robot localization based on ultra-wide-band ranging: A particle filter approach," Robotics Auton. Syst. **57** (2009) 496 (DOI: 10.1016/j.robot.2008.10.022).
[10] L. Taponecco, *et al.*: "Joint TOA and AOA estimation for UWB localization applications," IEEE Trans. Wireless Commun. **10** (2011) 2207 (DOI: 10.1109/TWC.2011.042211.100966).
[11] J. Wang, *et al.*: "Toward robust indoor localization based on Bayesian filter using chirp-spread-spectrum ranging," IEEE Trans. Ind. Electron. **59** (2012) 1622 (DOI: 10.1109/TIE.2011.2165462).
[12] N. A. Jones and S. V. Hum: "An ultra-wideband spatial filter for time-of-arrival localization in tunnels," IEEE Trans. Antennas Propag. **61** (2013) 5237 (DOI: 10.1109/TAP.2013.2272715).
[13] K. C. Ho: "Bias reduction for an explicit solution of source localization using TDOA," IEEE Trans. Signal Process. **60** (2012) 2101 (DOI: 10.1109/TSP.2012.2187283).
[14] J. M. Pak, *et al.*: "Improving reliability of particle filter-based localization in wireless sensor networks via hybrid particle/FIR filtering," IEEE Trans. Ind. Informat. **11** (2015) 1089 (DOI: 10.1109/TII.2015.2462771).
[15] J. M. Pak, *et al.*: "Distributed hybrid particle/FIR filtering for mitigating NLOS effects in TOA-based localization using wireless sensor networks," IEEE Trans. Ind. Electron. **64** (2017) 5182 (DOI: 10.1109/TIE.2016.2608897).
[16] D. Simon: *Optimal State Estimation: Kalman, H_∞, and Nonlinear Approaches* (John Wiley & Sons, Hoboken, NJ, 2006).
[17] B. Ristic, *et al.*: *Beyond the Kalman Filter: Particle Filters for Tracking Applications* (Artech House, Norwood, MA, 2004).
[18] J. M. Pak, *et al.*: "Horizon group shift FIR filter: Alternative nonlinear filter using finite recent measurements," Measurement **57** (2014) 33 (DOI: 10.1016/j.measurement.2014.07.007).
[19] J. M. Pak, *et al.*: "Weighted average extended FIR filter bank for managing horizon size in nonlinear FIR filtering," Int. J. Control. Autom. Syst. **13** (2015) 138 (DOI: 10.1007/s12555-014-0257-3).
[20] J. M. Pak, *et al.*: "Self-recovering extended Kalman filtering algorithm based on model-based diagnosis and resetting using an FIR filter," Neurocomputing **173** (2016) 645 (DOI: 10.1016/j.neucom.2015.08.011).
[21] J. M. Pak, *et al.*: "Switching extensible FIR filter bank for adaptive horizon state estimation with application," IEEE Trans. Control Syst. Technol. **24** (2016) 1052 (DOI: 10.1109/TCST.2015.2472990).
[22] J. M. Pak, *et al.*: "Fuzzy horizon group shift FIR filtering for nonlinear systems with Takagi-Sugeno model," Neurocomputing **174** (2016) 1013 (DOI: 10.1016/j.neucom.2015.10.029).
[23] J. M. Pak, *et al.*: "Self-recovering extended Kalman filtering algorithm based on model-based diagnosis and resetting using an FIR filter," Neurocomputing **173** (2016) 645 (DOI: 10.1016/j.neucom.2015.08.011).
[24] J. M. Pak, *et al.*: "Maximum likelihood FIR filter for visual object tracking," Neurocomputing **216** (2016) 543 (DOI: 10.1016/j.neucom.2016.07.047).
[25] J. M. Pak: "Memory parameterized FIR filtering for digital phase-locked loop," IEICE Electron. Express **16** (2019) 20181144 (DOI: 10.1587/elex.16.20181144).
[26] J. M. Pak, *et al.*: "Extended least square unbiased FIR filter for target tracking using the constant velocity motion model," Int. J. Control. Autom. Syst. **15** (2017) 947 (DOI: 10.1007/s12555-016-0572-y).
[27] J. M. Pak: "Gaussian sum FIR filtering for 2D target tracking," Int. J. Control. Autom. Syst. **18** (2020) 643 (DOI: 10.1007/s12555-018-0938-4).
[28] S. Blackman and R. Popoli: *Design and Analysis of Modern Tracking Systems* (Artech House, Norwood, MA, 1999).
[29] C. Musso, *et al.*: "Improving regularised particle filters," in *Sequential Monte Carlo Methods in Practice*, ed. A. Doucet, *et al.* (Springer, New York, NY, 2001).
[30] S. McGinnity and G. W. Irwin: "Multiple model bootstrap filter for maneuvering target tracking," IEEE Trans. Aerosp. Electron. Syst. **36** (2000) 1006 (DOI: 10.1109/7.869522).
[31] D. S. Angelova, *et al.*: "Application of Monte Carlo method for tracking maneuvering target in clutter," Math. Comput. Simul. **55** (2001) 15 (DOI: 10.1016/S0378-4754(00)00242-1).
[32] P. C. Mahalanobis: "On the generalised distance in statistics," Proc. of the National Institute of Sciences (1936).
[33] R. C. Smith and P. Cheeseman: "On the representation and estimation of spatial uncertainty," Int. J. Robot. Res. **5** (1986) 56 (DOI: 10.1177/027836498600500404).